Supersonic gas jet for fueling experiments on NSTX

V. A. Soukhanovskii¹, H. W. Kugel², R. Kaita², R. Majeski², A. L. Roquemore², D. P. Stotler²

¹Lawrence Livermore National Laboratory, Livermore, CA, USA ²Princeton Plasma Physics Laboratory, Princeton, NJ, USA

Introduction A new method for re-fueling a high temperature fusion plasma with a supersonic gas jet has been developed on the HL-1M tokamak [1] and later implemented on several nuclear fusion plasma facilities [2, 3]. The method favorably compares to the conventionally used fueling methods: subsonic gas injection at the plasma edge, and high velocity cryogenic fuel pellet injection into the plasma core. Experiments have demonstrated a fueling efficiency of 0.3 - 0.6, reduced interaction of injected gas with in-vessel components, and therefore a higher wall saturation limit, and a general simplicity of the method. Several models have been used to explain the enhanced penetration of the jet into the plasma: a cold channel model [4], an electrostatic double-layer shielding model [4], and a rapid plasma cooling leading to the increase in the ionization and dissociation length together with the polarization $\vec{E} \times \vec{B}$ drift [5]. However, the benefits of this new fueling method may be downgraded by its incompatibility with the high performance plasma regimes, namely the H-mode plasmas, and common auxiliary heating methods, such as the radio-frequency waves. To test and further optimize the concept, a supersonic gas injector (SGI) has been developed for the National Spherical Torus Experiment (NSTX) [6]. The NSTX Boundary Physics program presently focuses on edge power and particle flow optimization and control in high performance t < 1 s plasmas with auxiliary heating up to 12 MW [7]. The initial fueling of plasmas is achieved by injecting deuterium or helium through several fast piezoelectric valves with injection rates of up to 10²² particles/s, and a fueling efficiency of about 0.1 [8]. The fueling efficiency is defined as $\eta = (dN_i/dt) \Gamma_{qas}^{-1}$, where N_i is the confined particle inventory, and Γ_{gas} is the gas injecton rate. Experiments with the SGI planned for the near future will explore the compatibility of the supersonic gas jet fueling with H-mode single and double null diverted plasma scenarios, edge localized mode control, edge magnetohydrodynamic stability, radio frequency heating scenarios, and start-up scenarios with fast plasma density ramp-up. In a more distant future, the SGI can be used for plasma fueling with the planned active density control tools, such as cryopumping and low-recycling lithium surfaces.

Supersonic gas injector design and implementation The SGI is mounted on the NSTX vacuum vessel port slightly above the midplane (Fig. 1). It is comprised of a graphite nozzle and a modified Vecco PV-10 piezoelectric valve. A graphite shroud protects the assembly from the plasma. Integrated in the shroud are a flush-mounted Langmuir probe and two small magnetic coils for B_r and B_z measurements. The assembly is mounted on a Thermionics movable vacuum feedthrough controlled by a PC with a LabView interface. The SGI operates at room temperature. The most important part of the SGI is the supersonic nozzle. In principle, gas injection through any expansion (nozzle) can produce a supersonic jet if a pressure ratio between the nozzle reservoir and the background, P_0/P_{bg} is adequate as determined by the compressible fluid mechanics [9]. However, it is the nozzle geometry that determines supersonic jet properties, particularly the Mach number M. Several common nozzle shapes have been considered [6]. In comparison with a simple converging nozzle [1], a shaped Laval nozzle produces a highly uniform flow with constant Mach number, temperature, and density - the conditions favorable for molecular condensation. A higher flow intensity can be obtained with a lower pressure ratio in a contoured nozzle avoiding problems associated with normal Mach disk shocks. The significance of a high Mach number for the discussed applications is in two associated phenomena: Mach focusing and clustering (and condensation) of gas molecules. The Mach focusing is responsible for the formation of a low divergence high intensity jet.

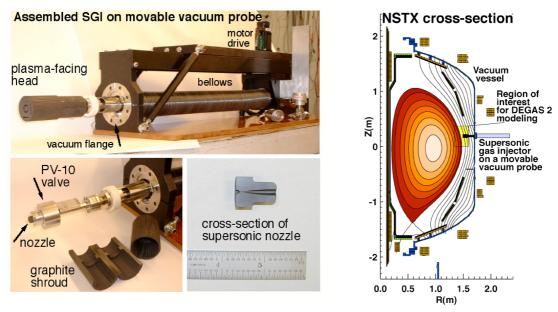


Figure 1: Supersonic gas injector layout and placement on the NSTX vacuum vessel

The molecular clustering may increase the jet density by orders of magnitude. It is characterized by an empirical Hangena parameter [10] for given nozzle parameters. The supersonic jet velocity is $u = Mc = M\sqrt{\gamma kT/m}$, c is a local speed of sound, and γ is the specific heat ratio. The static temperature T in a compressible flow, however, is reduced according to $T/T_0 = (1 + \frac{\gamma - 1}{2}M^2)^{-1}$, where T_0 is the stagnation temperature, so that the terminal velocity is $u_{max} = \sqrt{\frac{2 \gamma}{\gamma - 1}} \frac{kT_0}{m}$. The particle velocity distribution in the jet is described by a drifting narrowed Maxwellian distribution with the drift velocity u. Thus, the jet velocity u is only a factor of 2 - 3 greater than the thermal gas velocity $v_{th} = \sqrt{3kT_0/m}$. The Laval nozzle shape must be properly calculated to optimize the isentropic flow core and minimize the thickness of the boundary layer. This is usually done using the method of characteristics or computational fluid dynamics methodology based on numerical solution of the Navier-Stokes equations [9]. The nozzle geometry used in the NSTX SGI is a converging-diverging de Laval geometry. The geometry was obtained by scaling down by a factor of 60 a large wind tunnel nozzle operated in air $(\gamma = 1.401)$ at P = 1 atm and M = 8 [11]. The nozzle throat diameter is d = 0.254mm, the inlet diameter is 2.20 mm, and the exit diameter is 3.78 mm. The nozzle is 23.37 mm long (Fig.1). It was critical to evaluate the performance of the nozzle with different gases at the background pressure similar to the NSTX edge neutral pressure as the parameters of the jet core and the boundary layer do not scale similarly [12]. Another concern is that the SGI operates in a pulsed regime whereas any nozzle design relies on an established flow with steady-state parameters. The finite flow settle time limits the minimal SGI pulse length.

Results The goal of the characterization is to measure the gas injection rates, and to evaluate the gas jet profile, the flow Mach number, velocity, temperature and density. A local Mach number is obtained under the assumption of isentropicity from the Rayleigh - Pitot law using the pressure measurements upstream and downstream of the shock formed in front of the pressure transducer immersed in the flow:

$$\frac{P_i}{P_0} = \left(\frac{(\gamma+1) M^2}{(\gamma-1) M^2 + 2}\right)^{\gamma/(\gamma-1)} \left(\frac{\gamma+1}{2\gamma M^2 - (\gamma-1)}\right)^{1/(\gamma-1)} \tag{1}$$

The impact (stagnation) pressure P_i is measured on axis and the flow static pressure P_0 is measured in the SGI plenum [9]. The measurements [6] are designed to simulate the tokamak environment: the SGI injected gas pulses of 1 - 50 ms duration into a 50 liter vacuum tank

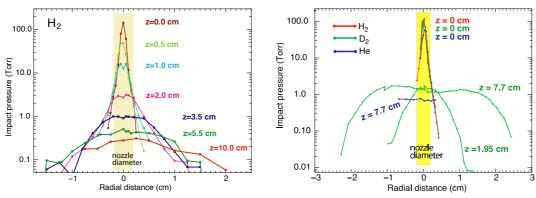


Figure 2: Measured jet impact pressure profiles with the nozzle PN-1 with hydrogen (left) and the nozzle PN-2 with hydrogen, deuterium and helium (right)

at the background pressure $P_b = 10^{-4}$ Torr, similar to the neutral pressures measured in NSTX. In the present set of measurements three gases have been used: hydrogen, deuterium, helium. The jet profile was found to be insensitive to the background pressure in the range $10^{-5} < P_h < 100$ Torr, consistent with the notion that the optimal background pressure for a supersonic expansion is equal to the static flow pressure. By varying the plenum pressure P_0 in the range from 300 to 3000 Torr, the injection rates from 0.25 to 1.5×10^{22} particles /s have been measured. Shown in Fig. 2 are the measured gas jet profile obtained at $P_0 \simeq 1000$ Torr corresponding to the injection rate of $S = 4.6 \times 10^{21}$ particles /s. Two identical nozzles PN-1 and PN-2 have been used, and the results are similar. The impact pressure profiles of hydrogen and deuterium are also similar, since the heat capacity ratios are 1.41 and 1.399, respectively. The central impact pressure of helium is smaller. Unlike the diatomic H₂ and D_2 molecules helium is a monatomic gas with $\gamma = 1.63$. The deduced Mach number at the nozzle exit is about 4 for deuterium, and about 6 for helium. When the deuterium pressure P_0 is lowered below 600 Torr the ratio P_0/P_i sharply decreases as the flow approaches sonic conditions. While the gas jet maintains its sharp density gradient for at least 120 mm, the measured central pressure sharply decreases at about 10 mm from the nozzle exit. This may be due to the flow underexpansion resulting from the improper scaling of the nozzle. From the isentropic flow relations one can estimate the jet core diameter corresponding to $M \simeq 4$: $A_*/A|_{M=4} \simeq 10$, from which $d_{core} \simeq 0.7$ mm is obtained. The boundary layer appears to be very thick, consistent with the measured profiles. The boundary layer thickness of the original Laval nozzle was measured to be 11.4 mm [11]. If it is scaled down by 60, the boundary layer of about 0.2 mm is obtained, a factor of 8 smaller than the one inferred from the measurements. The jet divergence half-angle is $\theta_{1/2} \simeq 6 - 12^{\circ}$. Using the isentropic relations between stagnation and static quantities [9] the density at the jet exit is estimated to be $\rho \leq 10^{18} \ \mathrm{cm}^{-3}$, and the temperature to be $T \geq 70 \ \mathrm{K}$. The nozzle Reynolds number is $Re \simeq 6000.$

Initial modeling of the supersonic gas jet has been performed using the Monte-Carlo neutral transport code DEGAS 2 and the 2D gas injection model described in [13]. Deuterium and helium injections into an L-mode plasma are simulated for the supersonic and conventional gas injectors. The supersonic jet in these simulations is prescribed the following parameters: diameter d=5 mm, temperature T=50 K, jet velocity v=2200 m/s, while T=300 K for the thermal gas injection. At present the simulations are not self-consistent and assume fixed background plasma temperatures and densities. The contour plots of the ion source rate and molecular density are shown in Fig. 3. In both cases the D₂ source rate of 5×10^{18} molecules/s has been used. The plots correspond to the rectangular region of interest shown in Fig. 1. Whereas the higher ion source rate and the density localization are apparent in the SGI case,

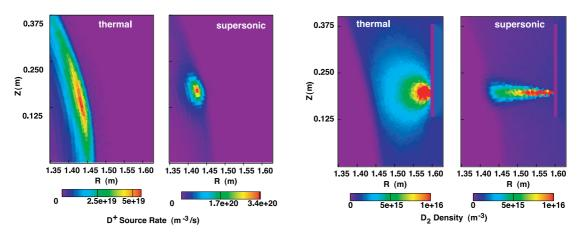


Figure 3: DEGAS 2 simulations of the thermal and supersonic gas injection: ion source rate (left) and molecular density (right) in the region of interest shown in Fig. 1

the penetration depth is similar for both fueling methods. The simulations will be compared to diagnostic data from the upcoming SGI fueling experiments and help quantify the fueling efficiency and neutral and ion source rate dynamics.

In summary, we have developed a pulsed supersonic gas injector for fueling and diagnostic applications on NSTX. The SGI utilizes a contoured Laval nozzle with the measured Mach number 4 for hydrogen and deuterium in a range of plenum pressures, a well defined density profile, and the divergence half-angle of $\theta_{1/2} \leq 12^o$. The measured SGI gas injection rate is up to 1.5×10^{22} particles/s. Future SGI development work will focus on the applications of the contoured nozzles designed for NSTX conditions. The diagnostic applications under consideration are the localized impurity gas injections for transport and turbulence experiments, and edge helium spectroscopy.

Acknowledgments We thank Prof. A. J. Smits and Dr S. Zaidi (Princeton University), W. Blanchard, G. Gettelfinger, T. Gray, L. Guttadora, T. Provost, P. Sichta, J. Taylor and J. Timberlake (PPPL) for their contributions to the project. This work is supported by the U.S. Department of Energy under Contracts No. W-7405-Eng-48 and DE-AC02-76CH03073.

^[1] L. Yao et al., Nuc. Fusion 41, 817 (July 2001).

^[2] B. Pegourie *et al.*, J. Nuc. Mater. **313-316**, 539 (2003).

^[3] J. Miyazawa et al., Nucl. Fusion **44**, 154 (2004).

^[4] J. Yiming, Z. Yan, Y. Lianghua, and D. Jiaqi, Plasma Phys. Control. Fusion 45, 2001 (2003).

^[5] J. Bucalossi et. al., in Proc. 29th Int Conf. on Fusion Energy, Lyon 2002 (IAEA, Vienna, 2002).

^[6] V. A. Soukhanovskii et al., Rev. Sci. Instrum. (accepted, 2004).

^[7] R. Maingi et al., Nuc. Fusion 43, 969 (2003.).

^[8] V. A. Soukhanovskii et al., J. Nuc. Mater. **313**, 573 (2003).

^[9] M. A. Saad, Compressible Fluid Dynamics (Prentice Hall, Englewood Cliffs, NJ, 1993).

^[10] O. F. Hagena, Rev. Sci. Instrum. **63**, 2374 (1992).

^[11] M. L. Baumgartner, Ph.D. thesis, Princeton University, 1997.

^[12] G. Dupeyrat, J. B. Marquette, and B. R. Rowe, Phys. Fluids 28, 1273 (1984).

^[13] D. P. Stotler *et al.*, Contrib. Plasma Phys. **44**, 3 (2004).